

# Measurement of the energy relaxation time of quantum states in quantum annealing with a D-Wave machine

Takashi Imoto\*

*Research Center for Emerging Computing Technologies,  
National Institute of Advanced Industrial Science and Technology (AIST),  
1-1-1 Umezono, Tsukuba, Ibaraki 305-8568, Japan.*

Yuki Susa<sup>†</sup> and Ryoji Miyazaki<sup>‡</sup>

*Secure System Platform Research Laboratories, NEC Corporation, Kawasaki, Kanagawa 211-8666, Japan and  
NEC-AIST Quantum Technology Cooperative Research Laboratory,  
National Institute of Advanced Industrial Science and Technology (AIST), Tsukuba, Ibaraki 305-8568, Japan*

Tadashi Kadowaki<sup>§</sup>

*DENSO CORPORATION, Kounan, Minato-ku, Tokyo 108-0075, Japan and  
Research Center for Emerging Computing Technologies,  
National Institute of Advanced Industrial Science and Technology (AIST),  
1-1-1 Umezono, Tsukuba, Ibaraki 305-8568, Japan.*

Yuichiro Matsuzaki<sup>¶</sup>

*Research Center for Emerging Computing Technologies,  
National Institute of Advanced Industrial Science and Technology (AIST),  
1-1-1 Umezono, Tsukuba, Ibaraki 305-8568, Japan. and  
NEC-AIST Quantum Technology Cooperative Research Laboratory,  
National Institute of Advanced Industrial Science and Technology (AIST), Tsukuba, Ibaraki 305-8568, Japan*

(Dated: February 22, 2023)

Quantum annealing has been demonstrated with superconducting qubits. Such a quantum annealer has been used to solve combinatorial optimization problems and is also useful as a quantum simulator to investigate the properties of the quantum many-body systems. However, the coherence properties of actual devices provided by D-Wave Quantum Inc. are not sufficiently explored. Here, we propose and demonstrate a method to measure the coherence time of the excited state in quantum annealing with the D-Wave device. More specifically, we investigate the energy relaxation time of the first excited states of a fully connected Ising model with a transverse field. We find that the energy relaxation time of the excited states of the model is orders of magnitude longer than that of the excited state of a single qubit, and we qualitatively explain this phenomenon by using a theoretical model. The reported technique provides new possibilities to explore the decoherence properties of quantum many-body systems with the D-Wave machine.

## I. INTRODUCTION

There have been significant developments in quantum annealing (QA). QA is useful to solve combinatorial optimization problems [1–3]. D-Wave Quantum inc. has developed a quantum annealing machine consisting of thousands of qubits [4]. It is possible to map the combinatorial optimization problem into the search for the ground state of the Ising Hamiltonian [5, 6]. Efficient clustering and machine learning using QA have been reported [7–14]. Moreover, QA can be used for topological data analysis (TDA)[15].

Furthermore, QA is used not only for solving problems but also as a quantum simulator of quantum many-

body systems in and out of equilibrium [16–19]. There is a great interest in whether the D-Wave machines exploit quantum properties, and recent experiments with a D-Wave machine have confirmed good agreement with theoretical predictions based on Schrodinger dynamics [20, 21]. Focusing on this point, an attempt has been reported to use longitudinal magnetic fields to probe the dynamics of a qubit and distinguish the effects of noise in the D-Wave machine[22]. However, the coherence properties of actual devices provided by D-Wave are not sufficiently explored, and further studies are still needed. In particular, since an eigenstate of the Hamiltonian provided by the D-Wave machine can be entangled, the coherence properties of entangled states need to be clarified.

In this paper, we propose and demonstrate a method to measure the energy relaxation time (called  $T_1$ ) of the excited states during QA by using the D-Wave machine. We adopt a fully connected Ising model of four qubits for the problem Hamiltonian of QA. We show that the energy relaxation time of the first excited states of the model is much longer than that of a single qubit. Our

---

\* takashi.imoto@aist.go.jp

† y-susa@nec.com

‡ miyazaki-aj@nec.com

§ tadashi.kadowaki.j3m@jp.denso.com

¶ matsuzaki.yuichiro@aist.go.jp

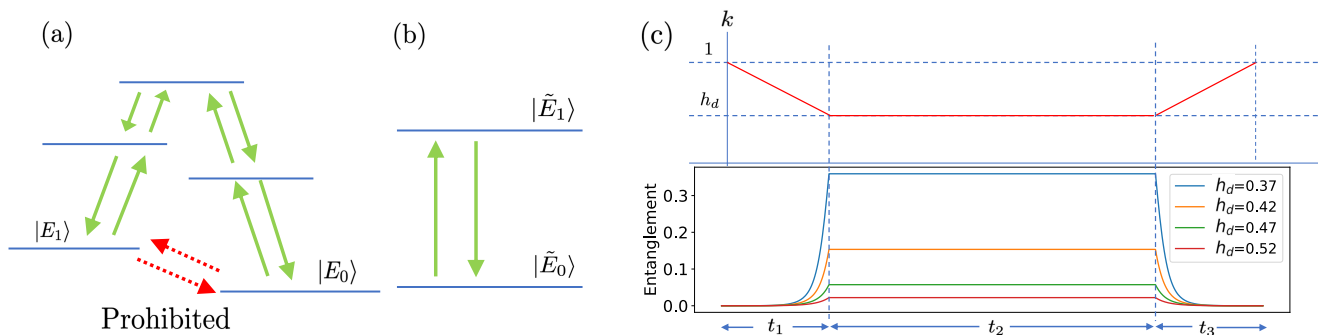


FIG. 1. (a) We illustrate the energy level diagram of the fully connected Ising model with the transverse field. For the small transverse magnetic field, we can use the lowest-order perturbation theory and obtain  $|E_0\rangle \approx |\downarrow\downarrow\downarrow\downarrow\rangle + \epsilon \sum_{j=1}^4 \sigma_j^{(+)} |\downarrow\downarrow\downarrow\downarrow\rangle$  and  $|E_1\rangle \approx |\uparrow\uparrow\uparrow\uparrow\rangle + \epsilon' \sum_{j=1}^4 \sigma_j^{(-)} |\uparrow\uparrow\uparrow\uparrow\rangle$  where  $\epsilon, \epsilon'$  denotes a small constant (see Appendix A). In this case, transition matrix elements of local operators between these states are zero. This means that the energy relaxation from  $|E_1\rangle$  to  $|E_0\rangle$  is unlikely for the lowest order perturbation, which indicates a long energy relaxation time under the effect of local noise. (b) We illustrate the energy level diagram of a single qubit. For some local operators, there are non-zero transition matrix elements between the ground state and the first excited state (see Appendix A). In this case, energy relaxation could occur under the effect of local noise unless the noise direction is completely parallel to the quantization axis. (c) The upper figure shows our scheduling of the reverse quantum annealing (RQA) to measure the energy relaxation time. Here,  $y$  axis represents an annealing parameter  $k$  to control the Hamiltonian in Eq. (1). The lower figure shows a calculated entanglement entropy of the state during RQA when the problem Hamiltonian is the fully connected Ising model. Our results show that the state during our protocol is entangled.

numerical simulations show that the first excited state during QA for the model is entangled, and so our experimental results indicate that the long-lived entangled state can be generated during QA with the D-Wave machine. Also, the energy diagram, which is illustrated in Fig 1 (a) and (b), can theoretically show that the fully-connected Ising model can lead to an improved energy relaxation time.

## II. EXPERIMENTAL RESULTS USING D-WAVE MACHINE

### A. $T_1$ Measurement Setup

Let us explain our method to measure the energy relaxation time of the excited states during QA by using the D-Wave machine. We perform the reverse quantum annealing (RQA) with a hot start where the initial state is the first excited state of the problem Hamiltonian, and we investigate the energy relaxation time of the state during RQA. We remark that, throughout this paper, we use the D-Wave Advantage system 6.1 for the demonstration. Although embedding techniques have been developed for a large number of qubits [23–29], we employ a fully connected Ising model with 4 qubits, which is the maximum system size without embedding. Moreover, we use several varieties of qubits in the D-Wave machine, and so we believe that our results are not limited to specific qubits but can be applied to general qubits in the D-Wave machine.

The Hamiltonian is given as follows:

$$H(k) = A(k)H_D + B(k)\left(g(k)H_L + H_P\right) \quad (1)$$

$$H_P = -J \sum_{j < k} \sigma_j^{(z)} \sigma_k^{(z)} \quad (2)$$

$$H_L = \frac{h}{2} \sum_{j=1}^N \sigma_j^{(z)} \quad (3)$$

$$H_D = -\Gamma \sum_{j=1}^N \sigma_j^{(x)}, \quad (4)$$

where  $H_P$  denotes the problem Hamiltonian,  $H_D$  denotes the drive Hamiltonian,  $H_L$  denotes the Hamiltonian of the longitudinal magnetic field,  $\Gamma$  ( $h$ ) denotes the amplitude of the transverse (horizontal) magnetic fields,  $J$  denotes the coupling strength,  $k$  denotes the time-dependent parameter to control the schedule of QA. We set  $A(k) = 1 - k$ ,  $B(k) = g(k) = k$ . Throughout our paper, we set  $h = 1$  and  $\Gamma = 1$  unless otherwise mentioned. Also, when we consider a fully connected Ising model, we set  $J = 1$  and  $N = 4$ . On the other hand, when we consider a non-interacting model (or a single-qubit model), we set  $J = 0$  and  $N = 1$  for simplicity. We choose the first excited state of the problem Hamiltonian, as an initial state. For the fully connected Ising model, the all-up state  $|\uparrow\uparrow\uparrow\uparrow\rangle$  is the excited state. The schedule of the Hamiltonian is described as follows. (See Fig. 1 (c)) Firstly, from  $t = 0$  to  $t = t_1$ , we change the parameter of the Hamiltonian from  $k = 1$  to  $k = h_d$  as a linear function of  $t$ , where we can control the strength of the transverse magnetic fields by tuning  $h_d$ . Secondly, from  $t = t_1$  to  $t = t_1 + t_2$ , we let the Hamiltonian remain

in the same form at  $k = h_d$ . Thirdly, from  $t = t_1 + t_2$  to  $t = t_1 + t_2 + t_3$ , we gradually change the parameter of the Hamiltonian from  $k = h_d$  to  $k = 1$ . Fourthly, we measure the state with a computational basis. Finally, we repeat this protocol with many different values of  $t_2$ . We obtain the survival probability of the initial state after these processes to estimate the energy relaxation time. Throughout this paper, the annealing times  $t_1$  and  $t_3$  are set to be  $1 \mu\text{s}$ .

### B. Experimental Result

By using our method described above, we measure the energy relaxation time of the first excited state. Moreover, we compare the energy relaxation time of the state of the transverse-field Ising model with that of the single-qubit model. Fig. 2 (a) shows the survival probability against  $t_2$  in the case of the fully connected Ising model with the transverse field. We can see that the survival probability decays exponentially. Furthermore, as we decrease  $h_d$ , the energy relaxation time becomes shorter. Fig. 2 (b) and (c) show the survival probability of the single-qubit model against  $t_2$ . Similar to the case of the fully connected Ising model, the coherence time becomes shorter as we decrease  $h_d$ . Importantly, the energy relaxation time of the state of the single-qubit model is shorter than that of the fully connected Ising model with the transverse field. The details of the experimental data about the measured energy relaxation time are shown in Appendix B. To gain our understanding of what occurs in the RQA, we separately perform numerical calculations. More specifically, we calculate the entanglement entropy of the first excited state during RQA when the problem Hamiltonian is the fully connected Ising model of four qubits. The entanglement entropy is defined by  $\text{Tr}[\rho_A \log \rho_A]$  where  $\rho_A$  denotes a reduced density matrix of the two qubits. We plot the results in 1 (c), and then find that the first excited state during QA is entangled if decoherence is negligible. The calculations also show that the entanglement entropy grows more for smaller  $h_d$ . Thus our results indicate that the energy relaxation time of the entangled state is longer than that of the separable state. We will discuss the origin of the long-lived state later.

In Fig. 3, we plot the survival probability against  $h_d$ . Again, we confirm that the survival probability of the case of the fully connected Ising model is larger than that of the non-interacting model. Although there is a tendency of the larger survival probability for smaller  $h_d$ , we observe that the survival probability becomes especially smaller for  $h_d = 0.43$  ( $h_d = 0.79$ ) for the case of the fully connected Ising model (non-interacting model). As we will discuss later, this is possibly due to noise sources at a specific frequency.

### III. DISCUSSION

Let us discuss the possible mechanism of the long-lived entangled states in our experiments. For a superconducting flux qubit composed of three Josephson junctions [30–32], which has been developed for a gate-type quantum computer, the main source of decoherence is the change in the magnetic flux penetrating the superconducting loop [33, 34]. This induces the amplitude fluctuation of  $\hat{\sigma}_z$ . Moreover, although the coherence time was not directly measured for the conventional RF SQUID, low-frequency flux noise was observed [35, 36], and the flux fluctuations induce the change in the amplitude of  $\hat{\sigma}_z$ . From the observations mentioned above, we infer that the qubits in the D-Wave machine are also affected by the amplitude fluctuation of  $\sigma_z$ . The energy relaxation rate of the first excited state typically increases as transition matrix  $|\langle g | \hat{\sigma}_j^{(z)} | e \rangle|$  increases [37] where  $|g\rangle$  and  $|e\rangle$  denote the ground and first excited state of the Hamiltonian, respectively. We numerically show that the transition matrix of the four qubits in the transverse-field Ising model is much smaller than that of a single qubit in the transverse and longitudinal fields Hamiltonian (See Fig. 4). This could be the origin of the long-lived entangled state during RQA. Also, to elucidate the mechanism, we analytically calculate the transition matrix by using a perturbation theory (see Appendix A).

In Fig. 3, we observe ‘bump’-like features around  $h_d = 0.43$  ( $h_d = 0.79$ ) for the case of the fully connected Ising model (single-qubit model), as we discussed before. The energy relaxation time becomes shorter for these values of  $h_d$ . For the superconducting qubit, it is known that two-level systems (TLSs) cause decoherence [38, 39], and the energy relaxation time can be smaller when the frequency of the qubit is resonant on that of the TLS [40–42]. We expect that the state during RQA is also affected by TLSs, and the energy relaxation time becomes smaller when the energy of the state is resonant with the TLS. By diagonalizing the Hamiltonian, we show that the energy gap between the ground and first excited states with  $h_d = 0.43$  for the fully connected Ising model is similar to that with  $h_d = 0.79$  for the single-qubit model (See Fig. 4 (b)). This result is consistent with our expectations that the bump structure is due to the TLS. Importantly, from these observations, our method to measure the energy relaxation time shows a potential to characterize the decoherence source during QA.

Let us compare our results to measure the energy relaxation time with previous results. In [43], the energy relaxation time of RF-SQUID with nonstoquastic interaction was measured, and the energy relaxation time is 17.5 ns, which is much shorter than that measured with our method by using a D-Wave machine. There are two possible reasons why the energy relaxation time in [43] is shorter than ours. First, to demonstrate a nonstoquastic Hamiltonian, they couple two qubits via charge and flux degrees of freedom. If there is a local basis to rep-

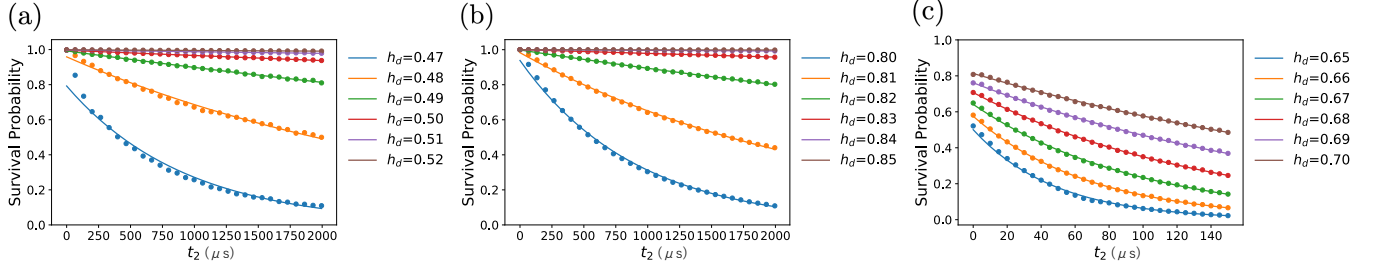


FIG. 2. (a) The survival probability against  $t_2$  for the fully connected Ising model ( $J = -1$ ) with the transverse field. The solid line shows a fitted exponential decay curve. (b) and (c) The survival probability against  $t_2$  for the single qubit. The solid line shows a fitted exponential decay curve. We set the fitting function to  $a \exp(-t/T_1)$  where  $T_1$  is the energy relaxation time and  $a$  is the constant factor. Each point is obtained with 100000 measurements. Also, we set  $t_1 = 1\mu\text{s}$ ,  $t_3 = 1\mu\text{s}$ , and  $h = 1.0$ .

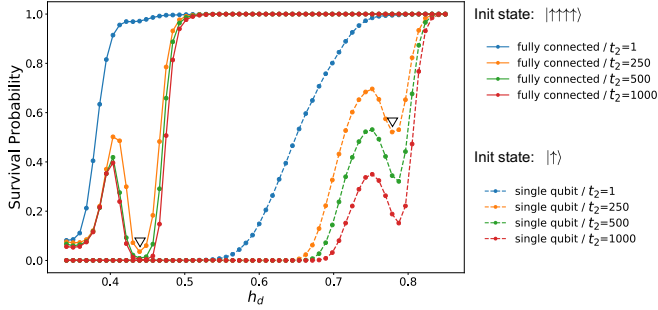


FIG. 3. The survival probability against  $h_d$  for the fully connected Ising model ( $J = -1$ ) with the transverse field and the single-qubit model. Each point is obtained with 100000 measurements. Also, we set  $t_1 = 1\mu\text{s}$ ,  $t_3 = 1\mu\text{s}$ , and  $h = 1.0$ . We observe ‘bump’-like features, which we indicate by using  $\nabla$ .

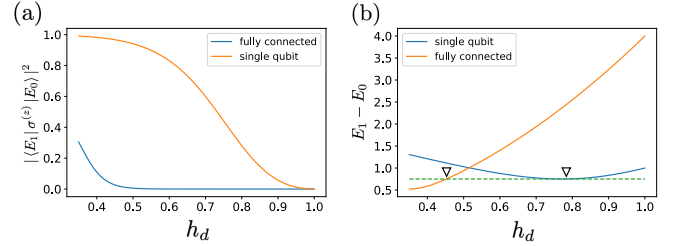


FIG. 4. Comparison between four qubits in the transverse-field Ising model and a single qubit in the transverse and longitudinal fields Hamiltonian. (a) Plot of the transition matrix of the noise operator  $\sigma^{(z)}$  between the ground state and first excited state. (b) Plot of the energy gap between the ground and the first excited states against  $h_d$ . From the results in Fig. 3, the energy relaxation time suddenly drops for the fully connected Ising model (single qubit model) when  $h_d = 0.45$  ( $h_d = 0.78$ ). The horizontal dashed line is a guide to the eye to show an energy gap of 0.75, and the energy gap of the fully connected Ising model (single qubit model) coincides with this value for  $h_d = 0.45$  ( $h_d = 0.78$ ), which we indicate by using  $\nabla$ . The figure suggests that there is a noise source to be resonant with the system when the energy gap is around 0.75.

represent the Hamiltonian whose off-diagonal elements are all positive, the Hamiltonian is called a stoquastic. The Hamiltonian in the D-Wave machine is stoquastic, because only inductive coupling is used. In [43], to utilize the charge degree for the nonstoquastic coupling, a more complicated structure is adopted, and this may decrease the energy relaxation time of the qubit. Second, when the energy relaxation time was measured in [43], they set a large tunneling energy corresponding to a transverse magnetic field such as 2 GHz. Here, the energy of the transverse magnetic field is much larger than that of the horizontal magnetic field. On the other hand, when we measure the energy relaxation time of the single qubit, the transverse magnetic field is smaller than the horizontal magnetic field, which makes the transition matrix  $|\langle g | \hat{\sigma}_j^{(z)} | e \rangle|$  smaller. These are the possible reasons why the energy relaxation time measured with our method is much longer than that in [43].

#### IV. CONCLUSION AND FUTURE WORK

In conclusion, we propose and demonstrate a method to measure the energy relaxation time of the first excited state during QA by using a D-Wave machine. We found that the energy relaxation time of the first excited state of the transverse-field Ising model is much longer than that of the single-qubit model. Using numerical simulations, we also find that the first excited state of the model is entangled. These findings indicate a long-lived entangled state during QA performed in the D-Wave machine. The origin of the long-lived entangled state was a small transition-matrix element of the noise operator between the ground state and the first excited state. Our work was regarded as the first proof-of-principle experiment of a direct measurement of the energy relaxation time of quantum states during QA with the D-Wave ma-

chine. Moreover, our results open new possibilities in the D-Wave machine to explore the coherence properties of the excited state of the quantum many-body systems.

This work was supported by Leading Initiative for Excellent Young Researchers MEXT Japan and JST presto (Grant No. JPMJPR1919) Japan. This paper is partly based on results obtained from a project, JPNP16007, commissioned by the New Energy and Industrial Technology Development Organization (NEDO), Japan. This work was supported by JST Moonshot R&D (Grant Number JPMJMS226C).

### Appendix A: Perturbative analysis for the long-lived qubit

As mentioned in the main text, the energy relaxation time of the first excited state of the fully connected Ising model with the longitudinal and transverse fields is much longer than that of a single qubit model. In order to elucidate the mechanism of its long energy relaxation time, we adopt the perturbation theory and obtain the explicit form of the ground state when the transverse magnetic field is small. This allows us to obtain the transition matrix, which is useful to quantify the robustness of the first excited state against decoherence [37].

We rewrite the total Hamiltonian (1) as

$$\begin{aligned} H &= H_0 + H' \\ H_0 &= H_P + H_L \\ H' &= \lambda \left( H_D - H_P - 2H_L + \lambda^2 H_L \right), \end{aligned} \quad (\text{A1})$$

where we set  $\lambda = 1 - k$  and  $\Gamma = 1$ . We can easily diagonalize  $H_0$ , and we assume that  $H'$  is a perturbative term.

Let us define  $\hat{S}^{(a)} = \sum_{j=1}^4 \hat{\sigma}_j^{(a)}$  ( $a = x, y, z$ ) and define  $S^{(z)}$  as the eigenvalue of  $\hat{S}_z$ . We consider the fully symmetric representation corresponding to the maximum total spin, and the subspace is spanned by the Dicke states. In this subspace, we can specify the state by  $S^{(z)}$ .

Using the perturbation theory, we can describe the  $n$ -th excited state as

$$|\phi_n\rangle = |\phi_n^{(0)}\rangle + \lambda \sum_{m \neq n} \frac{\langle \phi_m^{(0)} | H_D | \phi_n^{(0)} \rangle}{E_m^{(0)} - E_n^{(0)}} |\phi_m^{(0)}\rangle + o(\lambda^2), \quad (\text{A2})$$

where  $|\phi_m^{(0)}\rangle (E_m^{(0)})$  is  $m$ -th energy eigenstate (eigenenergy) of  $H_0$ , and we assume  $E_m \leq E_{m'}$  for  $m \leq m'$ . Here, we remark that  $|\phi_m^{(0)}\rangle$  is the computational basis, and so  $\langle \phi_n^{(0)} | H_L | \phi_m^{(0)} \rangle = \langle \phi_n^{(0)} | H_P | \phi_m^{(0)} \rangle = 0$  if  $m \neq n$ .

From Fig 1 (a), we obtain all the eigenstates as follows:

$$|\phi_0^{(0)}\rangle = |-4\rangle \quad (\text{A3})$$

$$|\phi_1^{(0)}\rangle = |+4\rangle \quad (\text{A4})$$

$$|\phi_2^{(0)}\rangle = |-2\rangle \quad (\text{A5})$$

$$|\phi_3^{(0)}\rangle = |+2\rangle \quad (\text{A6})$$

$$|\phi_4^{(0)}\rangle = |0\rangle. \quad (\text{A7})$$

Also, each energy eigenvalue is described as follows:

$$E_0^{(0)} = -8J - 2h \quad (\text{A8})$$

$$E_1^{(0)} = -8J + 2h \quad (\text{A9})$$

$$E_2^{(0)} = -2J - h \quad (\text{A10})$$

$$E_3^{(0)} = -2J + h \quad (\text{A11})$$

$$E_4^{(0)} = 0. \quad (\text{A12})$$

Substituting these values into the formula in Eq. (A2), we obtain an explicit form of the ground state and the first excited state as follows:

$$|\phi_0\rangle = |-4\rangle + \frac{\lambda}{6J+h} |-2\rangle + o(\lambda^2) \quad (\text{A13})$$

$$|\phi_1\rangle = |+4\rangle + \frac{\lambda}{6J-h} |+2\rangle + o(\lambda^2). \quad (\text{A14})$$

Note that these are entangled states. The transition matrix between the ground state and the first excited state is given by

$$\langle \phi_0 | \hat{\sigma}_j^{(z)} | \phi_1 \rangle = o(\lambda^2). \quad (\text{A15})$$

We can calculate the transition matrix of the other local operators. We obtain  $\langle \phi_0 | \hat{\sigma}_j^{(x)} | \phi_1 \rangle = o(\lambda^2)$  and  $\langle \phi_0 | \hat{\sigma}_j^{(y)} | \phi_1 \rangle = o(\lambda^2)$ . These show that this excited state is robust against the other local noise as well.

Similarly, we calculate the eigenvector of the single qubit model by using the perturbation theory for small transverse magnetic fields. The single qubit model is given by

$$H_{single} = \hat{\sigma}^{(z)} + \lambda \hat{\sigma}^{(x)}. \quad (\text{A16})$$

We describe the eigenstates as

$$|\psi_0\rangle = |\downarrow\rangle + \lambda |\uparrow\rangle + o(\lambda^2) \quad (\text{A17})$$

$$|\psi_1\rangle = |\uparrow\rangle + \lambda |\downarrow\rangle + o(\lambda^2), \quad (\text{A18})$$

where  $|\psi_0\rangle (|\psi_1\rangle)$  denotes the ground state (first excited state) of the single qubit. The transition matrix between the ground state and the first excited state is given by

$$\langle \psi_0 | \hat{\sigma}^{(z)} | \psi_1 \rangle = o(\lambda^1). \quad (\text{A19})$$

Comparing Eq. (A18) with Eq. (A15), we can confirm the first excited state of the the fully connected Ising model with the longitudinal and transverse field is more robust against noise represented by  $\hat{\sigma}_z$  than that of the single qubit model.

### Appendix B: Energy relaxation time

As described in the main text, we measured the energy relaxation time with the fully connected Ising model in the longitudinal and transverse fields and also measured that of the single-qubit model. Here, we show the details of the energy relaxation time of the fully connected Ising model in the longitudinal and transverse field (single-qubit model) in Table. I (II).

TABLE I. Energy relaxation time for each  $h_d$  for the fully connected Ising model( $J = -1$ )with the transverse field

$h_d$	energy relaxation time( $\mu s$ )
0.47	933.5
0.48	2991.0
0.49	10022.9
0.50	32729.6
0.51	104001.0
0.52	255612.5

TABLE II. Energy relaxation time for each  $h_d$  for the single qubit

$h_d$	relaxation time( $\mu s$ )
0.65	48.2
0.66	69.3
0.67	99.2
0.68	142.2
0.69	206.3
0.70	291.0
0.80	907.9
0.81	2426.6
0.82	9049.8
0.83	45920.6
0.84	262665.3
0.85	1032667.2

- 
- [1] T. Kadowaki and H. Nishimori, Quantum annealing in the transverse ising model, *Physical Review E* **58**, 5355 (1998).
- [2] E. Farhi, J. Goldstone, S. Gutmann, and M. Sipser, Quantum computation by adiabatic evolution, arXiv preprint quant-ph/0001106 (2000).
- [3] E. Farhi, J. Goldstone, S. Gutmann, J. Lapan, A. Lundgren, and D. Preda, A quantum adiabatic evolution algorithm applied to random instances of an np-complete problem, *Science* **292**, 472 (2001).
- [4] M. W. Johnson, M. H. Amin, S. Gildert, T. Lanting, F. Hamze, N. Dickson, R. Harris, A. J. Berkley, J. Johansson, P. Bunyk, *et al.*, Quantum annealing with manufactured spins, *Nature* **473**, 194 (2011).
- [5] A. Lucas, Ising formulations of many np problems, *Frontiers in physics* , 5 (2014).
- [6] W. Lechner, P. Hauke, and P. Zoller, A quantum annealing architecture with all-to-all connectivity from local interactions, *Science advances* **1**, e1500838 (2015).
- [7] K. Kurihara, S. Tanaka, and S. Miyashita, Quantum annealing for clustering, arXiv preprint arXiv:1408.2035 (2014).
- [8] V. Kumar, G. Bass, C. Tomlin, and J. Dulny, Quantum annealing for combinatorial clustering, *Quantum Information Processing* **17**, 1 (2018).
- [9] M. H. Amin, Searching for quantum speedup in quasistatic quantum annealers, *Physical Review A* **92**, 052323 (2015).
- [10] H. Neven, V. S. Denchev, G. Rose, and W. G. Macready, Training a binary classifier with the quantum adiabatic algorithm, arXiv preprint arXiv:0811.0416 (2008).
- [11] D. Korenkevych, Y. Xue, Z. Bian, F. Chudak, W. G. Macready, J. Rolfe, and E. Andriyash, Benchmarking quantum hardware for training of fully visible boltzmann machines, arXiv preprint arXiv:1611.04528 (2016).
- [12] M. Benedetti, J. Realpe-Gómez, R. Biswas, and A. Perdomo-Ortiz, Quantum-assisted learning of hardware-embedded probabilistic graphical models, *Physical Review X* **7**, 041052 (2017).
- [13] D. Willsch, M. Willsch, H. De Raedt, and K. Michielsen, Support vector machines on the d-wave quantum annealer, *Computer physics communications* **248**, 107006 (2020).
- [14] M. Wilson, T. Vandal, T. Hogg, and E. G. Rieffel, Quantum-assisted associative adversarial network: Applying quantum annealing in deep learning, *Quantum Machine Intelligence* **3**, 1 (2021).
- [15] J. J. Berwald, J. M. Gottlieb, and E. Munch, Computing wasserstein distance for persistence diagrams on a quantum computer, arXiv preprint arXiv:1809.06433 (2018).
- [16] A. D. King, J. Carrasquilla, J. Raymond, I. Ozfidan, E. Andriyash, A. Berkley, M. Reis, T. Lanting, R. Harris, F. Altomare, *et al.*, Observation of topological phenomena in a programmable lattice of 1,800 qubits, *Nature* **560**, 456 (2018).
- [17] P. Kairys, A. D. King, I. Ozfidan, K. Boothby, J. Raymond, A. Banerjee, and T. S. Humble, Simulating the

- shastri-sutherland ising model using quantum annealing, *PRX Quantum* **1**, 020320 (2020).
- [18] R. Harris, Y. Sato, A. Berkley, M. Reis, F. Altomare, M. Amin, K. Boothby, P. Bunyk, C. Deng, C. Enderud, *et al.*, Phase transitions in a programmable quantum spin glass simulator, *Science* **361**, 162 (2018).
- [19] S. Zhou, D. Green, E. D. Dahl, and C. Chamon, Experimental realization of classical z 2 spin liquids in a programmable quantum device, *Physical Review B* **104**, L081107 (2021).
- [20] A. D. King, S. Suzuki, J. Raymond, A. Zucca, T. Lanting, F. Altomare, A. J. Berkley, S. Ejtemaee, E. Hoskinson, S. Huang, *et al.*, Coherent quantum annealing in a programmable 2,000 qubit ising chain, *Nature Physics* **18**, 1324 (2022).
- [21] A. D. King, J. Raymond, T. Lanting, R. Harris, A. Zucca, F. Altomare, A. J. Berkley, K. Boothby, S. Ejtemaee, C. Enderud, *et al.*, Quantum critical dynamics in a 5000-qubit programmable spin glass, arXiv preprint arXiv:2207.13800 (2022).
- [22] Z. Morrell, M. Vuffray, A. Lokhov, A. Bärtschi, T. Albash, and C. Coffrin, Signatures of open and noisy quantum systems in single-qubit quantum annealing, arXiv preprint arXiv:2208.09068 (2022).
- [23] Z. Yang and M. J. Dinneen, *Graph minor embeddings for D-Wave computer architecture*, Tech. Rep. (Department of Computer Science, The University of Auckland, New Zealand, 2016).
- [24] S. Okada, M. Ohzeki, M. Terabe, and S. Taguchi, Improving solutions by embedding larger subproblems in a d-wave quantum annealer, *Scientific reports* **9**, 2098 (2019).
- [25] K. Boothby, P. Bunyk, J. Raymond, and A. Roy, Next-generation topology of d-wave quantum processors, arXiv preprint arXiv:2003.00133 (2020).
- [26] J. Cai, W. G. Macready, and A. Roy, A practical heuristic for finding graph minors, arXiv preprint arXiv:1406.2741 (2014).
- [27] C. Klymko, B. D. Sullivan, and T. S. Humble, Adiabatic quantum programming: minor embedding with hard faults, *Quantum information processing* **13**, 709 (2014).
- [28] T. Boothby, A. D. King, and A. Roy, Fast clique minor generation in chimera qubit connectivity graphs, *Quantum Information Processing* **15**, 495 (2016).
- [29] A. Zaribafiyani, D. J. Marchand, and S. S. Changiz Rezaei, Systematic and deterministic graph minor embedding for cartesian products of graphs, *Quantum Information Processing* **16**, 136 (2017).
- [30] I. Chiorescu, Y. Nakamura, C. M. Harmans, and J. Mooij, Coherent quantum dynamics of a superconducting flux qubit, *Science* **299**, 1869 (2003).
- [31] C. H. Van Der Wal, A. Ter Haar, F. Wilhelm, R. Schouten, C. Harmans, T. Orlando, S. Lloyd, and J. Mooij, Quantum superposition of macroscopic persistent-current states, *Science* **290**, 773 (2000).
- [32] J. Mooij, T. Orlando, L. Levitov, L. Tian, C. H. Van der Wal, and S. Lloyd, Josephson persistent-current qubit, *Science* **285**, 1036 (1999).
- [33] F. Yoshihara, K. Harrabi, A. Niskanen, Y. Nakamura, and J. S. Tsai, Decoherence of flux qubits due to  $1/f$  flux noise, *Physical review letters* **97**, 167001 (2006).
- [34] K. Kakuyanagi, T. Meno, S. Saito, H. Nakano, K. Semba, H. Takayanagi, F. Deppe, and A. Shnirman, Dephasing of a superconducting flux qubit, *Physical review letters* **98**, 047004 (2007).
- [35] T. Lanting, A. Berkley, B. Bumble, P. Bunyk, A. Fung, J. Johansson, A. Kaul, A. Kleinsasser, E. Ladizinsky, F. Maibaum, *et al.*, Geometrical dependence of the low-frequency noise in superconducting flux qubits, *Physical Review B* **79**, 060509 (2009).
- [36] R. Harris, J. Johansson, A. Berkley, M. Johnson, T. Lanting, S. Han, P. Bunyk, E. Ladizinsky, T. Oh, I. Perminov, *et al.*, Experimental demonstration of a robust and scalable flux qubit, *Physical Review B* **81**, 134510 (2010).
- [37] K. Hornberger, Introduction to decoherence theory, in *Entanglement and decoherence* (Springer, 2009) pp. 221–276.
- [38] R. W. Simmonds, K. Lang, D. A. Hite, S. Nam, D. P. Pappas, and J. M. Martinis, Decoherence in josephson phase qubits from junction resonators, *Physical Review Letters* **93**, 077003 (2004).
- [39] Y. Shalibo, Y. Rofe, D. Shwa, F. Zeides, M. Neeley, J. M. Martinis, and N. Katz, Lifetime and coherence of two-level defects in a josephson junction, *Physical review letters* **105**, 177001 (2010).
- [40] C. Müller, J. Lisenfeld, A. Shnirman, and S. Poletto, Interacting two-level defects as sources of fluctuating high-frequency noise in superconducting circuits, *Physical Review B* **92**, 035442 (2015).
- [41] P. Klimov, J. Kelly, Z. Chen, M. Neeley, A. Megrant, B. Burkett, R. Barends, K. Arya, B. Chiaro, Y. Chen, *et al.*, Fluctuations of energy-relaxation times in superconducting qubits, *Physical review letters* **121**, 090502 (2018).
- [42] L. V. Abdurakhimov, I. Mahboob, H. Toida, K. Kakuyanagi, Y. Matsuzaki, and S. Saito, Driven-state relaxation of a coupled qubit-defect system in spin-locking measurements, *Physical Review B* **102**, 100502 (2020).
- [43] I. Ozfidan, C. Deng, A. Smirnov, T. Lanting, R. Harris, L. Swenson, J. Whittaker, F. Altomare, M. Babcock, C. Baron, *et al.*, Demonstration of a nonstoquastic hamiltonian in coupled superconducting flux qubits, *Physical Review Applied* **13**, 034037 (2020).
- [44] K. Hornberger, Introduction to decoherence theory, *Entanglement and Decoherence: Foundations and Modern Trends*, 221 (2009).
- [45] J. Preskill, Quantum computing in the nisq era and beyond, *Quantum* **2**, 79 (2018).
- [46] A. Y. Kitaev, Fault-tolerant quantum computation by anyons, *Annals of Physics* **303**, 2 (2003).
- [47] B. M. Terhal, Quantum error correction for quantum memories, *Reviews of Modern Physics* **87**, 307 (2015).
- [48] S. J. Devitt, W. J. Munro, and K. Nemoto, Quantum error correction for beginners, *Reports on Progress in Physics* **76**, 076001 (2013).
- [49] P. W. Shor, Scheme for reducing decoherence in quantum computer memory, *Physical review A* **52**, R2493 (1995).
- [50] K. Bharti, A. Cervera-Lierta, T. H. Kyaw, T. Haug, S. Alperin-Lea, A. Anand, M. Degroote, H. Heimonen, J. S. Kottmann, T. Menke, *et al.*, Noisy intermediate-scale quantum algorithms, *Reviews of Modern Physics* **94**, 015004 (2022).